(Received 30 July 2024, Accepted 14 November 2024, Scheduled 27 November 2024)

The 6G Reconfigurable Reflectarray Antenna Using a Gold-VO-2 Bilayer Structure

Suhail Asghar Qureshi[1], Muhammad Ramlee Kamarudin[1,*], Muhammad Inam Abbasi[2], Yoshihide Yamada[3], Muhammad Hashim Dahri[4], Zuhairiah Zainal Abidin[1], and Nordin Ramli[5]

[1]*Faculty of Electrical and Electronic Engineering, Universiti Tun Hussein Onn Malaysia, Batu Pahat 86400, Malaysia*
[2]*Faculty of Electrical and Electronic Engineering Technology, Universiti Teknikal Malaysia Melaka Durian Tunggal 76100, Malaysia*
[3]*Malaysia Japan International Institute of Technology, Universiti Teknologi Malaysia Kuala Lumpur Jalan Semarak, Kuala Lumpur 54100, Malaysia*
[4]*Department of Telecommunication Engineering, Dawood University of Engineering and Technology Karachi 74800, Sindh, Pakistan*
[5]*MIMOS Berhad, Technology Park Malaysia, Kuala Lumpur 57000, Malaysia*

ABSTRACT: A reconfigurable reflectarray antenna (RRA) with beam steering capability at 1.1 THz is proposed. The element of reflectarray is composed of vanadium dioxide (VO-2) and a gold bilayer model designed on a unit cell of 0.45λ, in which temperature variations produce different reflection phases due to the dependence of VO-2 on ambient conditions. The proposed reflectarray antenna has an aperture of 3100 µm. When particular cells of the array are exposed to temperature over 340 K, it causes the phase in those unit cells to alter, eventually acting as 1-bit RRA. The radiation pattern shows a maximum gain of 24.3 dBi and a side lobe level of -14.4 dB with an aperture efficiency of 21.7%. The maximum gain in case of offset is over 21 dBi with sidelobe levels less than -10 dB up to 80-degree beam steering range. The proposed reconfigurable reflectarray antenna shows a beam steering capability of up to 100 degrees, which is sufficient for indoor communications. The designed antenna with its performance is optimum for the development of 6G RIS-based communication systems.

1. INTRODUCTION

The Terahertz (THz) band of frequencies (0.1 to 10 THz) is one of the most studied technologies in recent years, which can support ultra-high-speed wireless communications in future. Therefore, it is a promising option to address the limitation of communication system capacity and spectrum scarcity of current wireless systems. THz system, because of its ultrabroad bandwidth, can also assist proximal devices in sending/receiving data with ultrafast speed [1]. It can realize high-precision radar with low power consumption and compact size [2], and it can be used for spectroscopy and biological applications such as human body imaging [3]. Therefore, antennas with a gain of over 30 dBi are required in the THz band due to limited power levels. Conventional reflectors are usually used at low frequencies for high-gain applications, but they are costly for precise fabrication when being designed to operate at submillimetre-wave and THz frequencies [4]. On the other hand, reflectarray antennas are planar structures that combine the advantages of parabolic reflectors and phased array antennae [5]. The reflectarray antennas work as a reflection surface where the components of the array are responsible for the type of radiation pattern. The reflection coefficient magnitude and phase are significant factors in designing an array based on the position of particular unit cells [6]. It also suggests that the variation in each unit cell's properties can result in altered reflection patterns or directing the beam to a specific angle. Such a type of beam-scanning capability is critical to remote sensing and wireless communications [7]. The beam scanning is attained with the manipulation of the reflection characteristics of each unit cell electronically with the use of a phase shifter [8]. In [9], a PIN diode-based practical demonstration was proposed for the development of reconfigurable reflectarray working in X-band frequencies. Similarly, liquid crystal [10], varactor diode [11], and micro-electromechanical system (MEMS)-based systems [12] are used for designing the reconfigurable reflectarray. However, conventional phase-shifting techniques such as diode, liquid crystal, or MEMS-based systems are bulky phase shifters and cannot be integrated with terahertz systems. A possible THz reconfigurable technique was proposed in [13] that used graphene as a conducting patch of dimensions as low as $\lambda/16$. The graphene unit cells are designed at less than 0.1λ lattice area due to its plasmonic mode propagation. On the other hand, vanadium dioxide (VO-2) has also been studied for reconfigurability purposes. A metasurface for independent control mechanisms of transmit-reflectarray was proposed in [14] based on VO-2. An ultra-reconfigurable intelligent surface mechanism was proposed in [15] based on VO-2 for 5G applications. The study elaborated on the thermal and RF properties of the unit cell, and the feasibility of designing a recon-

* Corresponding author: Muhammad Ramlee Kamarudin (mramlee@uthm.edu.my).

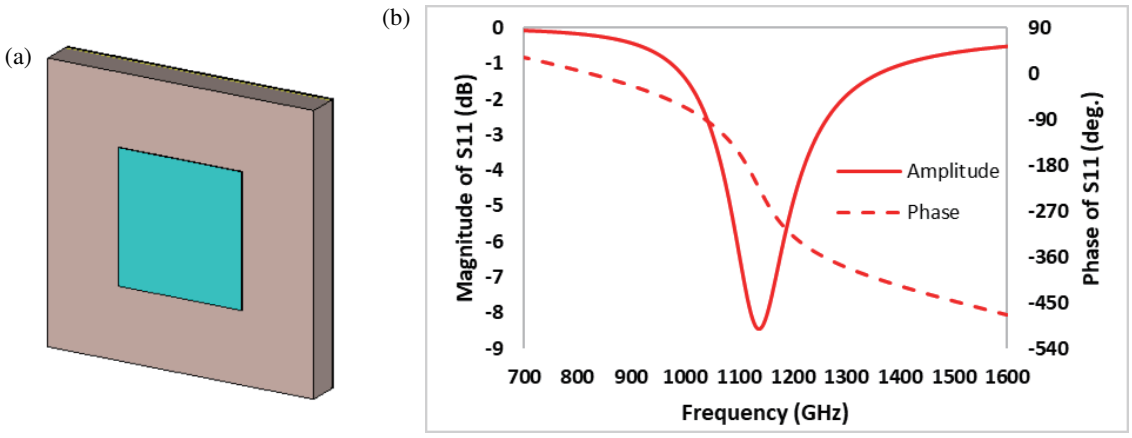

FIGURE 1. VO-2 based unit cell and (b) its reflection coefficient in the conductive state.

figurable intelligent surface was shown by the unit cell's operation at 32 GHz and 5 GHz. This suggests that the dependence of VO-2 conductivity on temperature is capable of being utilised in designing reconfigurable reflectarray for any frequency spectrum. Moreover, the concept of THz beam steering is still new and needs to be studied. Therefore, a VO-2-based reconfigurable reflectarray antenna has been proposed in this paper to address the challenge of beam steering at frequencies over 1 THz for communications. The proposed reflectarray is a bilayer model of gold and VO-2 structure in which temperature variations can alter the radiation pattern. The proposed RRA offers a 100-degree steering in beam, which is sufficient for indoor wireless communications at over 1 THz frequencies. This type of antenna can be integrated into the development of RIS-based 6G communications.

2. METHOD

2.1. VO-2 Characteristics

Vanadium dioxide can switch from a conductive state to an insulator state and vice versa, especially in the THz band. At room temperature, it exhibits the properties of an insulator, while it turns into a metal when the temperature exceeds its critical point of 340 K [14]. At temperatures lower than 340?,K, VO-2 remains insulating. The Drude model as given in (1) was used to model VO-2 as the dielectric material during simulations [16].

$$\varepsilon(\omega) = \varepsilon_{\infty} - \omega_p^2(\sigma)/\omega^2 + i\omega\gamma \tag{1}$$

where ε_{∞} represents the high-frequency permittivity that is 12 for VO-2; γ represents the damping frequency with the value of 5.75×10^{13} rad/s; and $\omega_p(\sigma)$ is the plasma frequency depending on conductivity. The plasma frequency's relationship with conductivity can be defined by (2) [14]:

$$\omega_p^2(\sigma) = \frac{\sigma}{\sigma_0}\omega_y^2(\sigma_0) \tag{2}$$

where σ_0 represents the absolute conductivity which is 3×10^5 S/m, and $\omega_y(\sigma_0)$ is the plasma frequency depending on absolute conductivity equal to 1.4×10^{14} rad/s [17]. The conductivity is typically a frequency dispersive variable, but it varies significantly according to temperature (T) in the case of VO-2 [14]. With the help of VO-2, a 1-bit reflection phase can be realized using its two distinct states, namely insulating and conducting. When the temperature is increased from 300 K to 400 K, the conductivity of VO-2 increases from 140 S/m to 5×10^5 S/m. This transition can be done in sub-picoseconds [18].

2.2. Why Bilayer?

Under the external stimulation of an electric field, heat or light pump, the conductivity of VO-2 can be increased to power orders of 4–5 magnitude. However, the conductivity of power 5 also accounts for losses in unit cells while working in THz frequencies compared to the conductivity of gold (4.09×10^7 S/m). Fig. 1(a) shows the typical element design of the reflectarray element with VO-2 as conducting patch and full ground. The reflection coefficient for VO-2 in a conductive state is less than -8 dB as shown in Fig. 1(b). This shows that less than 40% of power is reflected from VO-2, which is insufficient to design a reflectarray.

2.3. Unit Cell Design

The unit cell design as shown in Fig. 2 is a multilayered VO-2 and gold structure inspired by [19, 20]. A thin VO-2 sheet is designed on a substrate of polyimide that has a permittivity of 3.5. The thickness of the substrate (h) is 15 µm, and the VO-2 sheet thickness (vt) is 0.5 µm, while the ground and conducting patch of gold have a thickness (t) of 1 µm. The parallel strips of conducting patches of gold are modelled on top of the VO-2 layer. These strips of gold film can be fabricated on VO-2 by deposition of continuous gold with the process of physical vapour deposition [21]. The reflectarray is designed on inter-element spacing (a) of 125 µm, which is less than $\lambda/2$ (0.45λ) to ensure that grating lobes are minimum. The CST Studio software was used to model and perform analyses on the performance of the proposed unit cell. The perfect magnetic conductor (PMC) boundary was applied horizontally, and the perfect electric conductor (PEC) was applied vertically, whereas an incident elec-

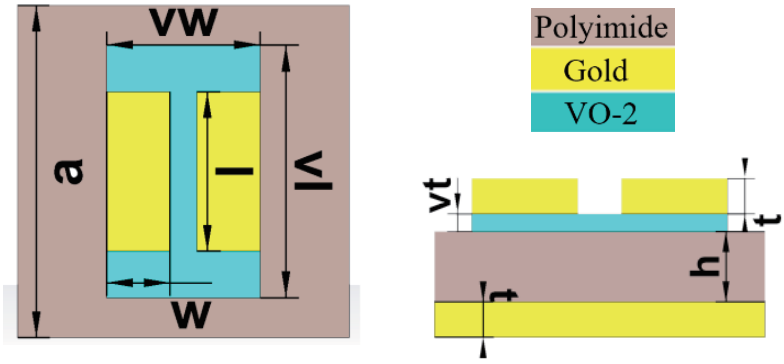

FIGURE 2. Schematic of the unit cell. $a = 125$ µm, $h = 15$ µm, $vl = 95$ µm, $vw = 58$ µm, $w = 24$ µm, $l = 60$ µm.

tromagnetic field was applied on the z-axis. The Frequency domain was used to simulate the unit cell designed in CST Studio. The designed unit cell was also simulated in the Ansys HFSS with primary and secondary boundary conditions in the x- and y-axis. A Floquet port was applied in the z-axis when simulating in HFSS.

First, the change in the reflection phase was determined versus conventionally changing the length of the parallel strips (l). The change in reflection coefficient with the change in dimension of the parallel strips at the desired frequency of 1100 GHz is represented by Fig. 3 with dotted lines showing the reflection phase of the unit cell and solid lines showing the reflection magnitude. It is realised that the change in dimensions of strips only causes shifting in resonance with the change in dimension of strips. The maximum reflection loss is found to be 3.0 dB when length (l) is 61 µm. This shows that 70% of the power is being reflected, which is optimum for designing of reflectarray. However, the reflection coefficient is not affected by a change in the length of parallel strips (l) when VO-2 switches to a conductive state. In this case, VO-2 acts as the conductor and a change in the dimension of another layer of the conductor (gold) will not affect the reflection coefficient.

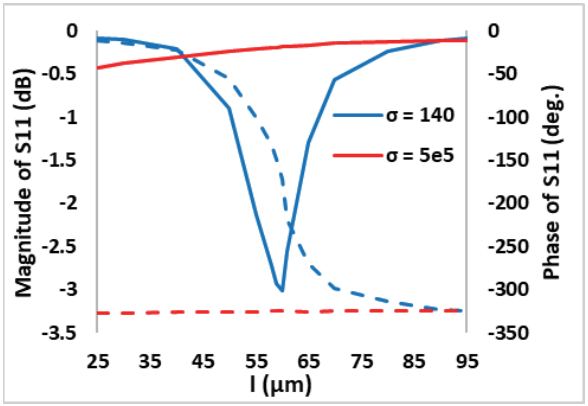

FIGURE 3. Reflection phase (- - -) and magnitude (—) at different conductivity states of VO-2 at 1100 GHz.

An experiment of reflectarray at this frequency is currently difficult due to fabrication and measurement challenges. A characterisation of the designed reflectarray would require equipment including the horn antenna and the VNA that are currently unavailable at the moment. Therefore, a comparison of CST and HFSS is made in Fig. 4. The simulated results in Fig. 4 with dotted lines represent the results obtained using HFSS, and the solid lines represent the results obtained using CST. More than 180° difference in reflection phase is apparent in S_{11} (represented by the solid black line) from 750 GHz to 1100 GHz when the conductivity depending on temperature is increased from 140 S/m to 5×10^5 S/m. Moreover, the resonance shifts from 1100 GHz to 740 GHz; therefore, the magnitudes at 1100 GHz for 300 K and 400 K are -3.01 dB and -0.19 dB, respectively. On the other hand, the reflection coefficient phase is 180° for the unit cell when it is at room temperature and goes to 360° when it is heated to 400 K. The process of heating the elements can be carried out with the help of micro heating elements, where it must be ensured that the VO-2 layer is evenly heated, and the gap of isolation is not smaller than the surface without VO-2 between adjacent unit cells. It was shown in a study conducted in [15] that 40×40 µm^2 heating elements required approximately 700 µm of gap to ensure thermal isolation between unit cells operating at 32 GHz. Since the dimensions of the VO-2 layer are 95×54 µm^2, the isolation required between unit cells would be 71 µm horizontally (a-vw) and 30 µm vertically (a-vl).

2.4. Reflectarray Design

The reflectarray antenna is typically a planar reflecting surface with several unit cells arranged on its aperture in such a way that the illuminating feed antenna produces a sharp reflecting beam. The distance travelled for the electromagnetic field (EMF) to reach the reflectarray aperture is different for each unit cell. Eventually, the EMF's phase for each unit cell is different, which is termed spatial phase delay. Thus, each element must compensate for the spatial phase delay depending on its position on the aperture so that a collimated beam can be produced. In the Cartesian coordinate system, the position of the i-th element can be represented as $(x_i,\ y_i)$, and (3) can be simplified for the collimated beam in the direction of (θ, φ) [22]:

$$\phi(\theta, \varphi) = \frac{2\pi}{\lambda}\left(R_i - \sin\theta\left(x_i \cos\varphi + y_i \sin\varphi\right)\right) - \pi\left(N + 1\right) \tag{3}$$

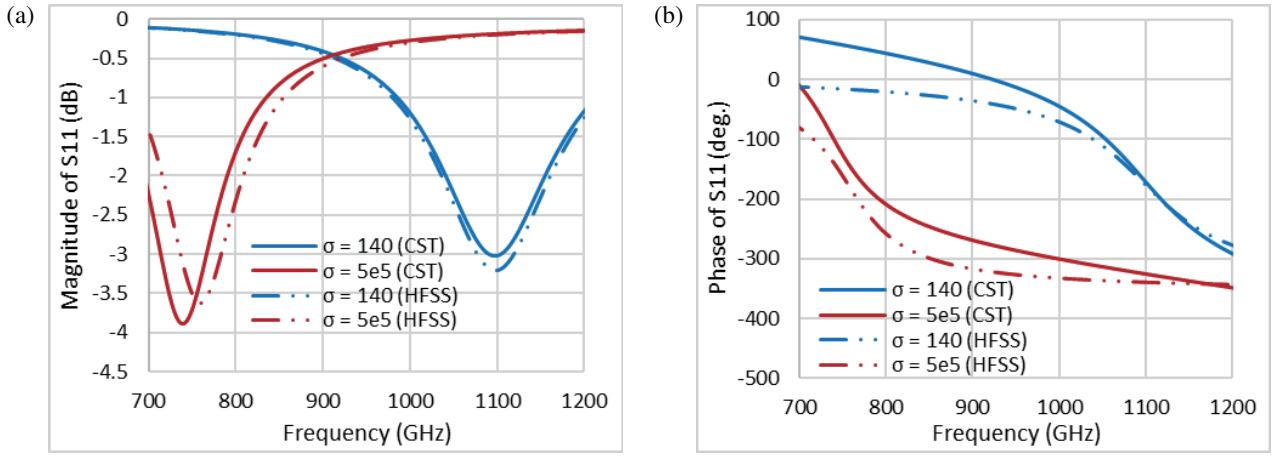

FIGURE 4. Comparison of reflection coefficient obtained using CST and HFSS (a) magnitude and (b) phase at different conductivity states of VO-2.

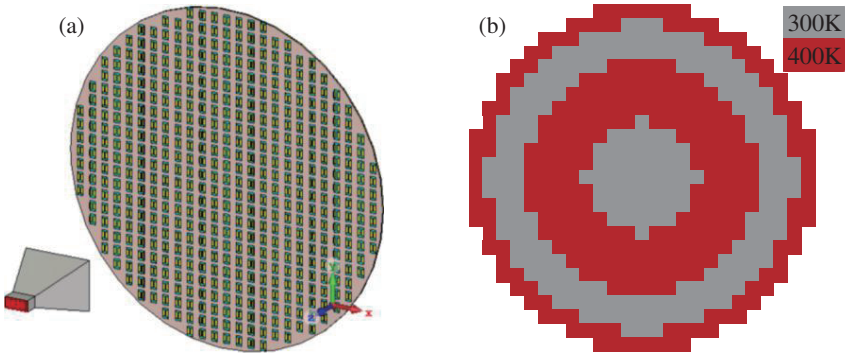

FIGURE 5. RRA design (a) array with feed and (b) 1-bit reflection phase configuration for pencil beam.

where $\phi(\theta, \varphi)$ is the spatial phase delay in degrees required for the i-th element; λ is the wavelength; N is the integer, which is the maximum number of elements on the horizontal or vertical axis; and R_i can be defined by (4):

$$R_i = \sqrt{(x_i - x_f)^2 + (y_i - y_f)^2 + z_f{}^2} \tag{4}$$

where x_f, y_f, and z_f are the coordinates of the feed antenna. It should be noted that if the calculated phase becomes positive for any unit cell of reflectarray, then it is subtracted by 360° until it becomes negative. In case the reflectarray is designed to operate as a mirror, θ and φ are set to 0° (normal to the surface of reflectarray), then (3) is reduced to:

$$\phi(0,0) = \frac{2\pi}{\lambda} R_i - \pi(N+1) \tag{5}$$

The required phase compensation can be achieved by either varying the conducting patch's length (l) or changing the reflection phase by changing the unit cells' electronic properties [23]. In this design, the properties of unit cells depend on the temperature.

3. RRA FOR BEAM STEERING

The designed reflectarray has a maximum number (N) of 489-unit cells. Fig. 5(a) shows the reflectarray, which is illuminated by the pyramidal feed antenna as done in [24]. The dimensions of the horn antenna and its radiation pattern are shown in Fig. 6. The distance between the feed antenna and reflectarray is set the same as the diameter of the reflectarray (Focal length to diameter ratio, $F/D = 1$) to ensure that the array elements at the edges are illuminated by -10 dB beamwidth of the pyramidal feed antenna. The flare length of the horn antenna is 600 µm. The array aperture is 3100 µm, and the -10 dB beamwidth of the feed antenna is 28°. Due to the limited reflectarray's aperture size, the elements at the edges make an angle of 28° with the feed reference of the horn antenna. The illumination efficiency of the design is determined to be 73%, while spillover efficiency is 93%. Generally, reflectarray requires continuous compensation of phase from 0° to 360°, but discrete states are used in practice. This leads to degradation in reflectarray performance, such as reduced aperture efficiency, bandwidth, gain, and increased sidelobe levels. The compensation phases are only $-180°$ and $-360°$, which represent the minimum phase difference of 180° required for the phase compensation method. It has been studied well that the radiation

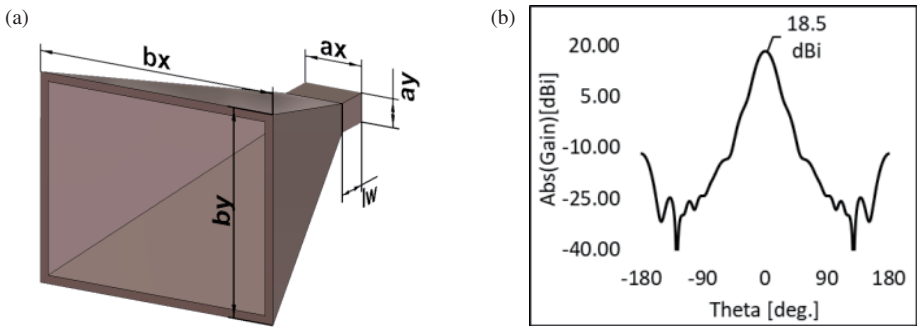

FIGURE 6. (a) pyramidal horn antenna (with dimensions $ax = 168\,\mu\text{m}$, $ay = 47\,\mu\text{m}$, $bx = 881\,\mu\text{m}$, $by = 715\,\mu\text{m}$, $lw = 136\,\mu\text{m}$) and (b) its radiation pattern.

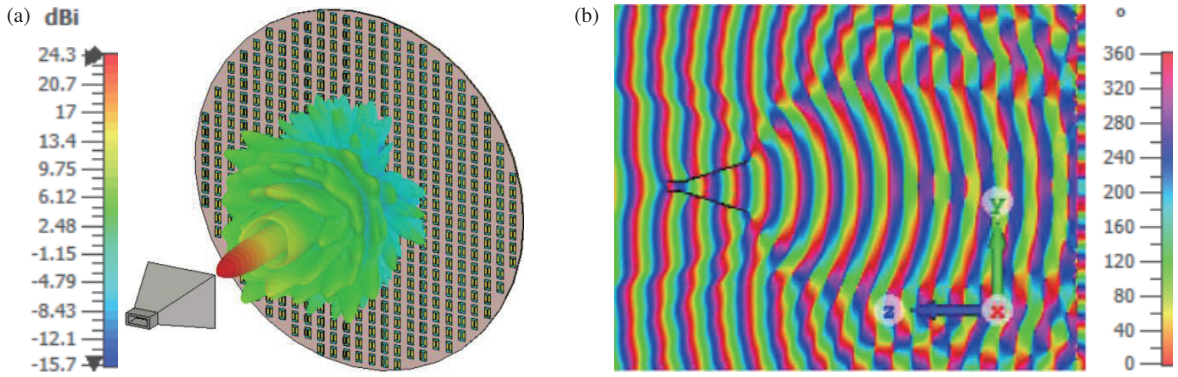

FIGURE 7. (a) Far-field pattern and (b) near-field phase distribution pattern.

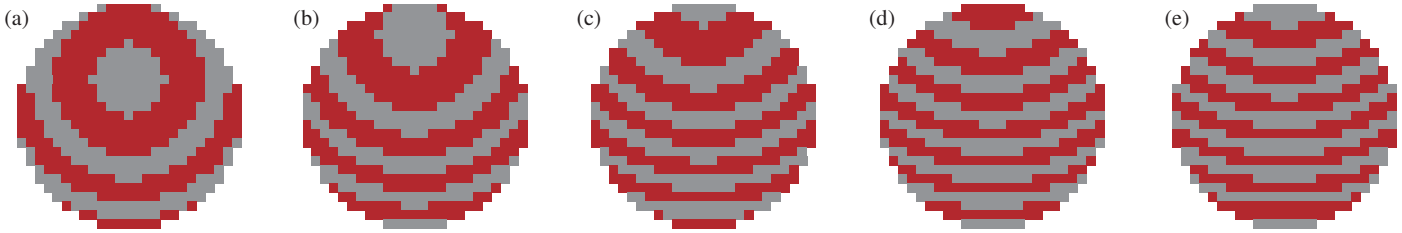

FIGURE 8. RRA phase configuration based on temperature for beam reflection to the angle of (a) 10°, (b) 20°, (c) 30°, (d) 40°, (e) 50°.

performance of reflectarrays using discrete phase compensation can be improved by increasing the size of the antenna, which requires a greater number of elements. The phase of reflection needed characteristics were calculated using Eq. (5), and the phase range calculated for 1-bit RRA is given by Eq. (6). The array is considered to be 1-bit reconfigurable, in which either the unit cell is heated to 400 K temperature, or it is at room temperature owing to the sudden transition of VO-2 from metal to insulator or vice versa. The red areas in phase configuration as shown in Fig. 5(b) represent the unit cells heated to 400 K, and the grey area represents the unit cells at room temperature. Full array simulations were carried out at frequencies from 900 GHz to 1200 GHz in the Time Domain Analysis of CST Studio. The boundary conditions were open (add space) in all directions. However, to reduce memory and time consumption, a hybrid module was used in Ansys HFSS to simulate the full reflectarray. The main lobe at 1100 GHz in the direction of $(\theta, \varphi) = (0, 0)$ has a gain of 24.3 dBi, and the sidelobe level is -14.4 dB as shown in Fig. 7(a). The reflectarray has an aperture efficiency of 21.7%, and the half-power (3 dB) beamwidth is found to be 5.1°. Fig. 7(b) shows the near-field phase distribution of the reflectarray, which is planar beyond the feed antenna. It verifies that the reflection coefficient phase requirement for the pencil beam has been obtained substantially.

$$\Phi = \begin{cases} -180^\circ, & -260 < \Phi < -100 \\ -360^\circ, & \text{Otherwise} \end{cases} \tag{6}$$

In the next step, several scenarios have been created for beam steering angle based on the characteristics of VO-2 that depend on temperature. Fig. 8 shows the configurations of the array for beamforming at different angles ranging from 10° to 50°.

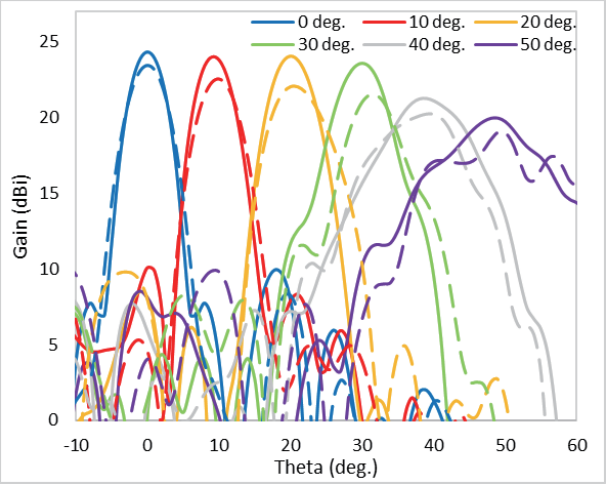

FIGURE 9. Comparison of radiation patterns of CST (—) and HFSS (- - -).

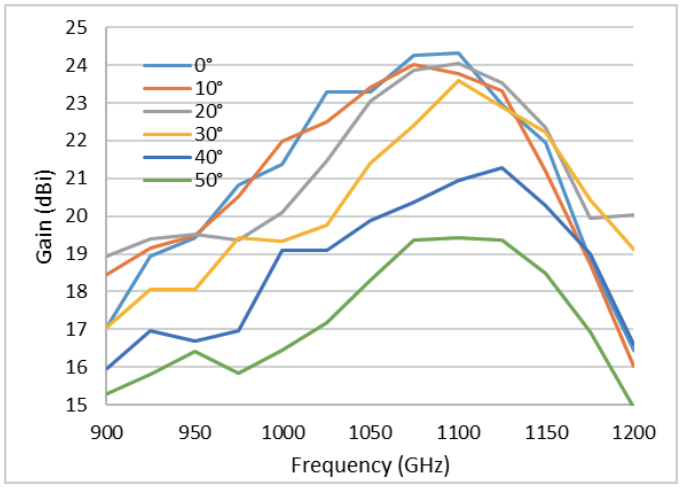

FIGURE 10. Bandwidth of designed RRA.

TABLE 1. Comparison of the state-of-the-art RRAs.

Ref.	Freq (GHz)	Phase shifter element	Number of elements	Maximum Gain (dBi)	Beam scanning range (°)	Aperture efficiency (%)	Function
[24]	115	Liquid crystal	1521	16.55	20	-	Beam-Scanning
[27]	1600	Graphene	13,600	17.8	-	-	OAM
[5]	800-850	Graphene	169	22.6	-	40	Frequency tuning
[28]	100	Liquid crystal	2,200	19.4	55	18.5	Beam-Scanning
[29]	108	Liquid crystal	400	24.3	90	-	Beam-Scanning
This work	1100	VO-2	489	24.3	100	21.7	Beam-Scanning

The phase centre of reflectarray is moved up to form an angle from the feed antenna. Therefore, beam steering is realised at phi $= 90°$, and theta varies from 0 to 50°. A comparison of the radiation patterns obtained for the designed phase configurations using CST and HFSS is shown in Fig. 9. The highest gain using HFSS (dashed lines) was found to be slightly lower than the highest gain obtained using CST (solid lines) for each phase configuration. This error can be attributed to the slight mismatch found in the reflection coefficient results. Fig. 9 shows that the designed reflectarray beam can be steered up to $\pm 30°$ in the h-plane with sidelobe levels less than -10 dB and deviation in the main lobe less than 1 dB. When the beam steering angle is at theta $= \pm 40°$, the gain decreases to 21 dBi. At about theta $= \pm 50$, the gain drops below 20 dBi, and sidelobe levels are greater than -10 dB.

Figure 10 shows the gain over frequency of the designed RRA. It was observed from the plot that the normalized gain is more than -1 dB between 1025 GHz and 1125 GHz, which makes up 9% of the bandwidth according to the centre frequency of 1100 GHz. However, as the steering angles increase, the bandwidth of the antenna represents a decline. Table 1 presents a comparison of previously designed RRA with state-of-the-art designs. Most of the reconfigurable reflectarrays at over 100 GHz operate based on the liquid crystal as a phase shifter element. Liquid crystals show a large birefringence, which has been employed successfully for phase shifting in microwave and millimetre wave frequencies previously [25]. However, it was shown in [26] that nematic liquid crystals (NLCs) at over 1 THz frequency exhibit a small extinction coefficient and comparatively large birefringence. Graphene was used in [5, 27] for the generation of vortex waves and the designing of frequency tuneable reflectarray, respectively. In contrast to the previously proposed RRAs, the presented design shows beam scanning at a frequency range of over 1 THz with high efficiency. With such efficiency and beam steering capabilities, the proposed structure has the potential to be integrated into the development of 6G RIS-base communication systems.

4. POTENTIAL FABRICATION PROCESS AND SENSITIVITY ANALYSIS

The potential fabrication process consists of two main stages. In the first stage, the VO2 disc needs to be grown and shifted to the substrate. The VO2 layer can be prepared by hot pressing the VO2 power [30]. This process begins with placing graphite die inside a glove box containing Ar gas. VO2 powder is collected inside a graphite die which is hot pressed at different temperatures (450–1000°C) for two minutes at a pressure around

100 MPa. Later, the VO2 layer needs to be shifted to the polyimide substrate. In the second stage, the gold layer needs to be fabricated on top of the VO2 layer, which can be done through wet-etching [31]. Initially, a 1 µm thick layer of gold needs to be splutter-coated onto the surface of a Polyimide followed by a photoresist layer applied, spin-coated, exposed and processed to define the required pattern. Later, the excess gold needs to be removed using an acid solution. Finally, any remaining photoresist can be removed using acetone. The results are predictive using CST and HFSS until it is feasible to experiment. For this reason, a geometrical error test is carried out to show the tolerance error in the fabrication of the proposed reflectarray. With regards to the defects that may occur during the fabrication, a tolerance from 1.25% to 10% on the dimensions of the unit cell "l", "vl", "w" and "vw" was done in reflectarray design. As shown in Fig. 11, the highest tolerance in terms of "l", "vl", "w" and "vw" was found to be 1.25%, 5%, 2.5%, and 10%, respectively so that the drop in the highest gain is as low as 1 dB.

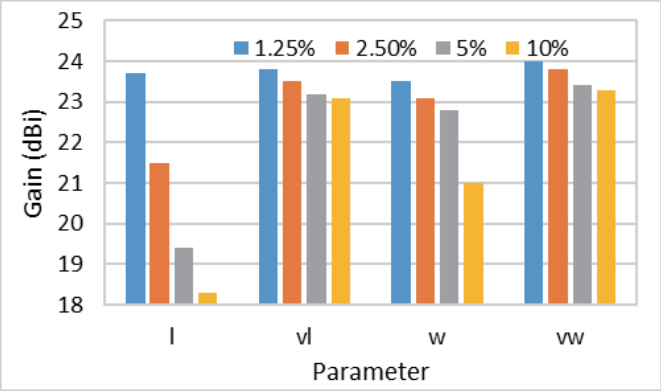

FIGURE 11. Highest gain of RRA on variation in dimensions.

5. CONCLUSION

This work proposes a novel unit cell based on a bilayer model of gold and VO-2 structure designed on a polyimide substrate to manipulate the radiation pattern of reflectarray. A phase difference of more than 180° is experienced by the unit cell on the variation of temperature from 300 K to 400 K. A reflectarray comprising a maximum of 489 unit cells is illuminated by a pyramidal horn antenna. The variation in temperature on the unit cells causing phase manipulation steers the beam in different directions. The simulated results showed a maximum gain of 24.3 dBi with an aperture efficiency of 21.7% at theta angle of 0 degrees. In the case of temperature variation, an offset at a theta angle of $\pm 50°$ is realised whose main lobe has a magnitude of over 21 dBi with side lobe levels of less than -10 dB. The proposed reflectarray has a high gain at 0° like a broadside array, and multiple beams are realized in the case of offset, which is significant for applications such as terahertz wireless communications in indoor communication. This can also be employed in the development of 6G RIS-based communications.

STATEMENTS AND DECLARATIONS

Competing Interests: The authors declare that they have no conflict of interest.

Funding Statement: This research was supported by Ministry of Higher Education (MOHE) through Fundamental Research Grant Scheme (FRGS) (FRGS/1/2021/TK0/UTHM/02/19).

REFERENCES

[1] Yang, F., P. Pitchappa, and N. Wang, "Terahertz reconfigurable intelligent surfaces (RISs) for 6G communication links," *Micromachines*, Vol. 13, No. 2, 285, Feb. 2022.

[2] Wang, J., M. Naftaly, and E. Wasige, "An overview of terahertz imaging with resonant tunneling diodes," *Applied Sciences*, Vol. 12, No. 8, 3822, Apr. 2022.

[3] Niu, T., W. Withayachumnankul, B. S.-Y. Ung, H. Menekse, M. Bhaskaran, S. Sriram, and C. Fumeaux, "Experimental demonstration of reflectarray antennas at terahertz frequencies," *Optics Express*, Vol. 21, No. 3, 2875–2889, 2013.

[4] Miao, Z.-W., Z.-C. Hao, Y. Wang, B.-B. Jin, J.-B. Wu, and W. Hong, "A 400-GHz high-gain quartz-based single layered folded reflectarray antenna for terahertz applications," *IEEE Transactions on Terahertz Science and Technology*, Vol. 9, No. 1, 78–88, Jan. 2019.

[5] Zainud-Deen, S. H., A. M. Mabrouk, and H. A. Malhat, "Frequency tunable graphene metamaterial reflectarray for terahertz applications," *The Journal of Engineering*, Vol. 2018, No. 9, 753–761, 2018.

[6] Tayebi, A., J. Tang, P. R. Paladhi, L. Udpa, S. S. Udpa, and E. J. Rothwell, "Dynamic beam shaping using a dual-band electronically tunable reflectarray antenna," *IEEE Transactions on Antennas and Propagation*, Vol. 63, No. 10, 4534–4539, 2015.

[7] Xi, B., Y. Xiao, K. Zhu, Y. Liu, H. Sun, and Z. Chen, "1-bit wideband reconfigurable reflectarray design in Ku-band," *IEEE Access*, Vol. 10, 4340–4348, 2021.

[8] Mei, P., S. Zhang, and G. F. Pedersen, "A low-cost, high-efficiency and full-metal reflectarray antenna with mechanically 2-D beam-steerable capabilities for 5G applications," *IEEE Transactions on Antennas and Propagation*, Vol. 68, No. 10, 6997–7006, 2020.

[9] Abbasi, M. I., M. Y. Ismail, and M. R. Kamarudin, "Development of a pin diode-based beam-switching single-layer reflectarray antenna," *International Journal of Antennas and Propagation*, Vol. 2020, No. 1, 8891759, 2020.

[10] Li, X., Y. Wan, J. Liu, D. Jiang, T. Bai, K. Zhu, J. Zhuang, and W.-Q. Wang, "Broadband electronically scanned reflectarray antenna with liquid crystals," *IEEE Antennas and Wireless Propagation Letters*, Vol. 20, No. 3, 396–400, 2021.

[11] Baladi, E., M. Y. Xu, N. Faria, J. Nicholls, and S. V. Hum, "Dual-band circularly polarized fully reconfigurable reflectarray antenna for satellite applications in the Ku-band," *IEEE Transactions on Antennas and Propagation*, Vol. 69, No. 12, 8387–8396, 2021.

[12] Perruisseau-Carrier, J. and A. K. Skrivervik, "Monolithic MEMS-based reflectarray cell digitally reconfigurable over a 360° phase range," *IEEE Antennas and Wireless Propagation Letters*, Vol. 7, 138–141, 2008.

[13] Carrasco, E. and J. Perruisseau-Carrier, "Reflectarray antenna at terahertz using graphene," *IEEE Antennas and Wireless Propagation Letters*, Vol. 12, 253–256, 2013.

[14] Li, T., H. Wang, F. Ling, Z. Zhong, and B. Zhang, "High-efficiency terahertz metasurface with independently controlled

and switchable function in transmission and reflection modes," *Superlattices and Microstructures*, Vol. 146, 106653, 2020.

[15] Matos, R. and N. Pala, "VO2-based ultra-reconfigurable intelligent reflective surface for 5G applications," *Scientific Reports*, Vol. 12, No. 1, 4497, 2022.

[16] Scarfe, S., W. Cui, A. Luican-Mayer, and J.-M. Ménard, "Systematic THz study of the substrate effect in limiting the mobility of graphene," *Scientific Reports*, Vol. 11, No. 1, 8729, 2021.

[17] Zhao, Y., Q. Huang, H. Cai, X. Lin, and Y. Lu, "A broadband and switchable VO2-based perfect absorber at the THz frequency," *Optics Communications*, Vol. 426, 443–449, 2018.

[18] Zhou, R., T. Jiang, Z. Peng, Z. Li, M. Zhang, S. Wang, L. Li, H. Liang, S. Ruan, and H. Su, "Tunable broadband terahertz absorber based on graphene metamaterials and VO2," *Optical Materials*, Vol. 114, 110915, 2021.

[19] Squires, A. D., X. Gao, J. Du, Z. Han, D. H. Seo, J. S. Cooper, A. T. Murdock, S. K. H. Lam, T. Zhang, and T. Van Der Laan, "Electrically tuneable terahertz metasurface enabled by a graphene/gold bilayer structure," *Communications Materials*, Vol. 3, No. 1, 56, 2022.

[20] Lee, S.-G., Y.-H. Nam, Y. Kim, J. Kim, and J.-H. Lee, "A wide-angle and high-efficiency reconfigurable reflectarray antenna based on a miniaturized radiating element," *IEEE Access*, Vol. 10, 103 223–103 229, Sep. 2022.

[21] Thomas, A., P. Savaliya, K. Kumar, A. Suchitta, and A. Dhawan, "Au nanowire-VO2 spacer-Au film based optical switches," *Journal of the Optical Society of America B*, Vol. 35, No. 7, 1687–1697, 2018.

[22] Hassan, A. A., R. R. Elsharkawy, D. A. Saleeb, E.-S. M. El-Rabie, and A. S. Elkorany, "Single-beam graphene reflectarray for terahertz band communication," *Analog Integrated Circuits and Signal Processing*, Vol. 112, No. 3, 517–525, 2022.

[23] Huang, J. and J. A. Encinar, *Reflectarray Antennas*, John Wiley & Sons, 2007.

[24] Yang, J., P. Wang, S. Sun, Y. Li, Z. Yin, and G. Deng, "A novel electronically controlled two-dimensional terahertz beam-scanning reflectarray antenna based on liquid crystals," *Frontiers in Physics*, Vol. 8, 576045, Oct. 2020.

[25] Lim, K. C., J. D. Margerum, and A. M. Lackner, "Liquid crystal millimeter wave electronic phase shifter," *Applied Physics Letters*, Vol. 62, No. 10, 1065–1067, Mar. 1993.

[26] Hsieh, C.-F., R.-P. Pan, T.-T. Tang, H.-L. Chen, and C.-L. Pan, "Voltage-controlled liquid-crystal terahertz phase shifter and quarter-wave plate," *Optics Letters*, Vol. 31, No. 8, 1112–1114, 2006.

[27] Chang, Z., B. You, L.-S. Wu, M. Tang, Y.-P. Zhang, and J.-F. Mao, "A reconfigurable graphene reflectarray for generation of vortex THz waves," *IEEE Antennas and Wireless Propagation Letters*, Vol. 15, 1537–1540, 2016.

[28] Perez-Palomino, G., M. Barba, J. A. Encinar, R. Cahill, R. Dickie, P. Baine, and M. Bain, "Design and demonstration of an electronically scanned reflectarray antenna at 100 GHz using multiresonant cells based on liquid crystals," *IEEE Transactions on Antennas and Propagation*, Vol. 63, No. 8, 3722–3727, Aug. 2015.

[29] Meng, X., M. Nekovee, and D. Wu, "The design and analysis of electronically reconfigurable liquid crystal-based reflectarray metasurface for 6G beamforming, beamsteering, and beamsplitting," *IEEE Access*, Vol. 9, 155 564–155 575, 2021.

[30] Dahal, K., Q. Zhang, R. He, I. K. Mishra, and Z. Ren, "Thermal conductivity of (VO2) 1-xCux composites across the phase transition temperature," *Journal of Applied Physics*, Vol. 121, No. 15, 155103, 2017.

[31] Wang, B., A. Sadeqi, R. Ma, P. Wang, W. Tsujita, K. Sadamoto, Y. Sawa, H. R. Nejad, S. Sonkusale, C. Wang, M. Kim, and R. Han, "Metamaterial absorber for THz polarimetric sensing," in *Terahertz, RF, Millimeter, and Submillimeter-Wave Technology and Applications XI*, Vol. 10531, 170–176, Feb. 2018.